

## Involvement of p21 and FasL in Induction of Cell Cycle Arrest and Apoptosis by Neochamaejasmin A in Human Prostate LNCaP Cancer Cells

Wing-keung Liu,<sup>\*,†</sup> Florence W. K. Cheung,<sup>†</sup> Bonnie P. L. Liu,<sup>†</sup> Chunman Li,<sup>†</sup> Wencai Ye,<sup>‡</sup> and Chun-Tao Che<sup>§</sup>

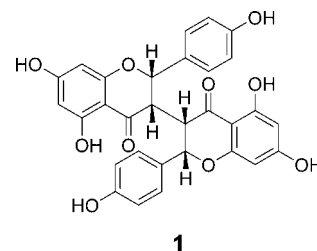
Department of Anatomy, Faculty of Medicine, The Chinese University of Hong Kong, Shatin, N.T., Hong Kong, People's Republic of China, School of Chinese Medicine, The Chinese University of Hong Kong, Shatin, N.T., Hong Kong, People's Republic of China, and Institute of Traditional Chinese Medicine and Natural Products, Jinan University, Guangzhou 510632, People's Republic of China

Received February 25, 2008

Neochamaejasmin A (**1**), a biflavonoid isolated from the roots of a traditional Chinese medicine, *Stellera chamaejasme* L., was shown to inhibit cellular <sup>3</sup>H-thymidine incorporation (IC<sub>50</sub> 12.5 μg/mL) and subsequent proliferation of human prostate cancer LNCaP cells. Treatment of LNCaP cells with low doses of **1** (≤6.25 μg/mL) suppressed DNA-binding activities of the transcription factors NFκB and AP-1 to the promoter of cyclin D and also inhibited expression of the cell cycle regulatory proteins cyclin D, proliferating cell nuclear antigen, and nucleolin, thus arresting cells in G<sub>1</sub> phase of the cell cycle. A lengthy exposure with higher doses of **1** (≥12.5 μg/mL) revealed the production of reactive oxygen species, dissipation of the mitochondrial membrane potential, up-regulation of cyclin-dependent kinase inhibitor p21, and induction of cell apoptosis. An aggregation of Fas–procaspase 8–procaspase 3 and p21–procaspase 3 proteins by coimmunoprecipitation, immunoblotting analysis, and MALDI-mass spectrometry indicated the involvement of Fas and p21 in **1**-mediated cytotoxicity, and pretreatment of cells with antisense FasL oligonucleotides partially abolished apoptosis. Thus, **1** blocked cell cycle progression at the G<sub>1</sub> phase by activating the p21 protein and ultimately promoting the Fas–caspase 8–caspase 3 apoptotic machinery.

Dutasteride is a drug that reduces the availability of the physiologically potent dihydrotestosterone by more than 90% and consequently induces prostatic epithelial apoptosis and atrophy.<sup>1</sup> A number of substances, including nonsteroidal anti-inflammatory drugs<sup>2</sup> and flavonoids,<sup>3</sup> have been reported to induce apoptosis in human prostate cancer cells, either through a receptor-dependent pathway involving an interaction between a ligand and its receptor such as FasL and Fas that activates caspase 8<sup>4,5</sup> or through a receptor-independent pathway by which an association of drastic reactive oxygen species generation with the activation of cyclin-dependent kinase inhibitors p53/p21 leads to an opening of the mitochondrial transition pore, the release of the apoptosis-inducing factor, and translocation of cytochrome *c* from mitochondria into the cytosol for triggering apoptosis.<sup>3</sup>

“Lang-Du” is a toxic Chinese herbal medicine claimed to possess chemotherapeutic properties.<sup>6</sup> This herbal drug is derived from the dried roots of any one of three plant species, namely, *Stellera chamaejasme* L., *Euphorbia fischeriana* Steud., or *Euphorbia ebracteolata* Hayata.<sup>7</sup> Chemical investigations on these medicinal plants have led to the isolation of sterols, triterpenes, tannins, and a number of diterpene compounds,<sup>7–9</sup> and the ethanolic and aqueous extracts of *E. fischeriana* and *S. chamaejasme* were found to inhibit the growth of Lewis lung carcinoma and ascitic hepatoma in mice.<sup>10</sup> We have shown the growth inhibition (IC<sub>50</sub> 40 μM) and neuroendocrine differentiation of LNCaP cells by jolkinolide b, a diterpene isolated from *E. fischeriana*.<sup>11</sup> Substantial evidence has demonstrated the antiproliferative activity of flavonoids on LNCaP cells, but no information is available for biflavonoids. In the present study, we have demonstrated that **1**, a biflavonone constituent of dried roots of *S. chamaejasme*, arrested cell progression at the G<sub>1</sub> phase, preceding induction of apoptosis in human LNCaP cells through the Fas–caspase 8–caspase 3 pathway, which provides a better understanding of the cytotoxic properties of this biflavonone.



### Results and Discussion

Previously, we have isolated 10 pure compounds from the roots of *S. chamaejasme* for a preliminary cytotoxic screen by colorimetric tetrazolium MTT assay, and the results revealed that **1**, a biflavonoid with a C-3/C-3'' linkage, possessed the most potent in vitro cytotoxicity.<sup>12,13</sup> Since biflavonoids have reported anti-inflammatory, antiviral, cytotoxic, and antioxidative properties,<sup>14–16</sup> the toxicity of **1** was further determined among three tumor cell lines, and the IC<sub>50</sub> values were 12.5, 25.1, and 90 μg/mL for LNCaP cells, human colon SW620 carcinoma cells, and mouse L929 fibroblasts, respectively, indicating that the LNCaP cells were most sensitive to **1** (IC<sub>50</sub> 12.5 μg/mL = 23 μM) (Figure 1a). The antiproliferative activity was confirmed by a <sup>3</sup>H-Tdr incorporation assay (Figure 1b), and it was considered that this interesting property warranted detailed mechanistic studies in LNCaP cells.

Normal LNCaP cells are spindle-shaped with a central nucleus and formed loosely adherent colonies on the surface of the culture plate (Figure S1a, Supporting Information). Mitochondria with closely packed cristae were scattered in the cytoplasm (Figure S1b, Supporting Information). After treatment with ≤12.5 μg/mL of **1**, the cytoplasmic processes retracted and the cells became round-shaped with many vacuoles in the cytoplasm. The mitochondria were swollen with reduced matrix density and degraded cristae, while the chromatin condensed, revealing a nuclear morphology typical for apoptosis that occurred at a dose-dependent manner (Figure S1c–e, Supporting Information). Cells completely lost surface structure and started to die at ≥12.5 μg/mL (Figure S1f, Supporting Information). Nucleolin, a major nucleolar protein involved in ribosome biosynthesis, was visible as dots in the nucleus of the untreated and exponentially proliferating cells (Figure S1g,

\* To whom correspondence should be addressed. Tel: (852) 2609-6896. Fax: (852) 2603-5031. E-mail: ken-liu@cuhk.edu.hk.

<sup>†</sup> Faculty of Medicine, The Chinese University of Hong Kong.

<sup>‡</sup> Jinan University.

<sup>§</sup> School of Chinese Medicine, The Chinese University of Hong Kong.

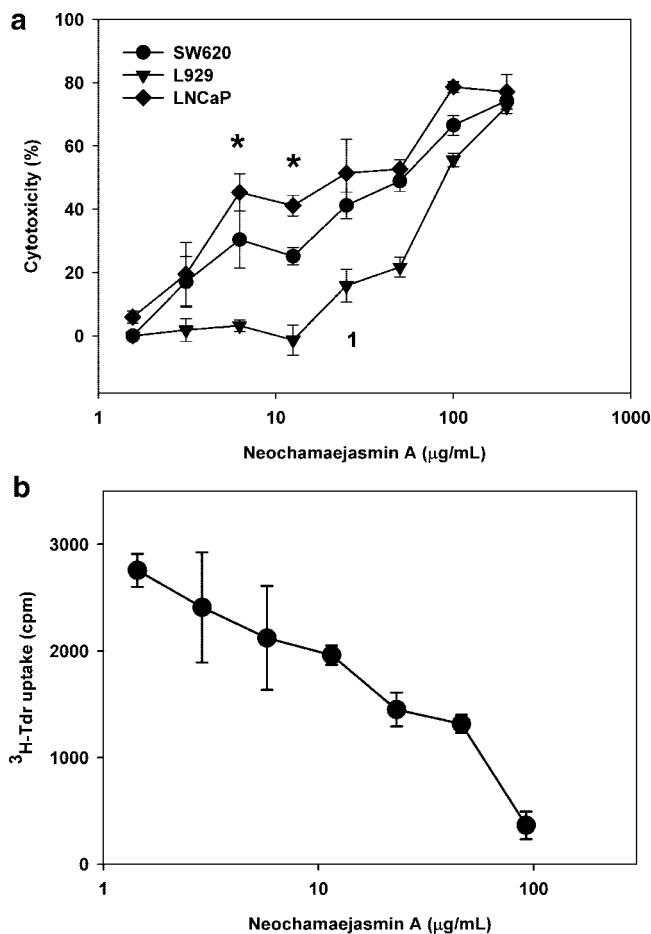


**Figure 1.** Cytotoxicity of **1** on different cancer cell lines as determined by the MTT assay (a). The human prostate LNCaP cancer cell line was the most susceptible to **1** treatment, and the  $IC_{50}$  was  $12.5 \mu\text{g/mL}$  ( $23 \mu\text{M}$ ), as determined by a  $^3\text{H}$ -thymidine uptake method (b). Data points represent the mean values and standard deviations of triplicate samples.

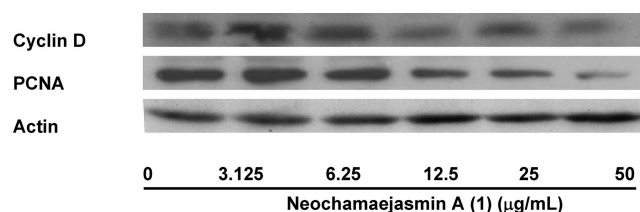


**Figure 2.** Immunoblotting analysis of cell proliferation proteins was shown in LNCaP cells after **1** treatment for 48 h (a). Equal amounts of proteins in the cell lysate from each treatment group were subjected to gel electrophoresis and immunoblotted with antibodies against cyclin D and PCNA. Both proteins decreased significantly ( $p < 0.05$ ) at doses  $\geq 6.25 \mu\text{g/mL}$  **1** (b). Data are mean and standard error of one experiment repeated three times with essentially similar results. Significant variation between treatment doses was determined using one-way analysis of variance followed by Duncan's test ( $p < 0.05$  compared with untreated control).

Supporting Information), but decreased dramatically and disappeared in cells after exposure to **1**, a feature that has also been reported in apoptotic cells.<sup>17</sup>

When LNCaP cells were exposed to low doses of **1** ( $6.25$  to  $12.5 \mu\text{g/mL}$ ) for 24 h, the levels of cyclin D and PCNA, two major  $G_1$  regulatory proteins, decreased in a dose-dependent manner (Figure 2). Cyclin D1 expression was suppressed through a mechanism involving a reduced binding of the transcription factors AP-1 and NF $\kappa$ B to their specific elements in the cyclin D promoter,

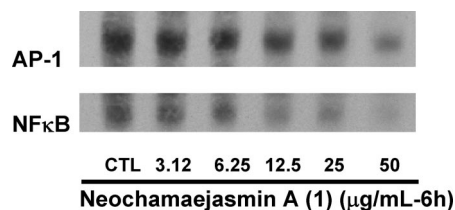


**Figure 3.** Electrophoretic mobility shift assay (EMSA) demonstrating the binding of nuclear proteins from **1**-treated cells to biotin-labeled cyclin D-specific activation protein-1 (AP-1) and NF $\kappa$ B oligonucleotides. Competition with 200-fold molar excess of unlabeled probes demonstrated the specificity of the bands, and no DNA binding was observed in untreated cells (data not shown).

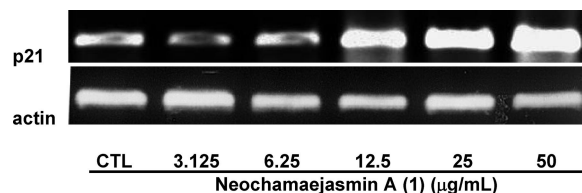


**Figure 4.** RT-PCR analysis showing significant transcriptional increase ( $p < 0.05$ ) of the cyclin-dependent kinase inhibitor gene, p21, in LNCaP cells treated with **1** ( $> 12.5 \mu\text{g/mL}$ ) for 24 h. Results are presented as average of three experiments and standard deviations. Significant variation between treatment doses was determined using one-way analysis of variance followed by Duncan's test ( $p < 0.05$  compared with untreated control).

as measured by an electrophoretic mobility shift assay (Figure 3).<sup>18</sup> In addition, an increase of p21 transcript was also found in LNCaP cells using a semiquantitative RT-PCR assay (Figure 4). p21<sup>Waf1/Cip1</sup>, a cyclin-dependent kinase inhibitor, belongs to the Cip/Kip family (p21<sup>Waf1/Cip1</sup>, p27<sup>Kip1</sup>, and p57<sup>Kip2</sup>), which exhibits both antiproliferative and antiapoptotic activities. It controls cell cycle progression by binding to cyclin D, an activating protein for Cdk4 in the  $G_1$  phase, and PCNA, an auxiliary protein required for replicative enzyme DNA polymerase  $\delta$  during DNA synthesis and repair.<sup>19,20</sup> In human diploid fibroblasts, p21 has been shown to interact with cyclin, CDK, and PCNA to form quaternary complexes for cell cycle progression or growth arrest machinery.<sup>14,19,21</sup> Results of a kinetic cell cycle analysis on normal untreated LNCaP cells using flow cytometry revealed that 60% of normal LNCaP cells were in the  $G_1$  phase at days 1, 3, and 5, and at 70% at days 2, 4, and 6, indicating that a cell cycle of LNCaP cells was around 2 days.<sup>11</sup> In contrast,  $6.25 \mu\text{g/mL}$  **1** gradually arrested cells at the  $G_1$  phase, namely, 75% of the cells after 4 days, with less than 10% of the cells proceeding to the S phase. When the cells were incubated with higher doses of **1** ( $> 6.25 \mu\text{g/mL}$ ) for 48 h, the  $G_1$  population was reduced significantly ( $p < 0.05$ ) in a dose-dependent manner, with a concomitant increase of sub $G_1$  population, indicating an induction of apoptosis in LNCaP cells (Figure S2, Supporting Information).

Reactive oxygen species, including superoxide anion, hydroxyl radicals, and hydrogen peroxides, are byproducts of normal aerobic metabolism in the human body, and they are produced mainly in the mitochondria, endoplasmic reticulum, plasma membrane, and cytosolic organelles.<sup>13</sup> These oxidative species not only participate in antimicrobial defense mechanisms<sup>15</sup> but are also involved in cell signal transduction, initiation of cytochrome *c* release, and modulation of transcription factor expression (e.g., NF $\kappa$ B and AP-1) that link to apoptosis.<sup>22,23</sup> The generation of ROS was activated by **1** for 30 min, starting from a median fluorescence intensity of 4.8 in the untreated control, increasing by 1.5-fold and 3.5-fold at  $6.25$  and  $50 \mu\text{g/mL}$ , respectively (Figure 5a). Concomitant with this oxidative stress, the mitochondrial membrane potential decreased by 1.6-fold at  $6.25 \mu\text{g/mL}$  and to only half at  $50 \mu\text{g/mL}$  for 18 h

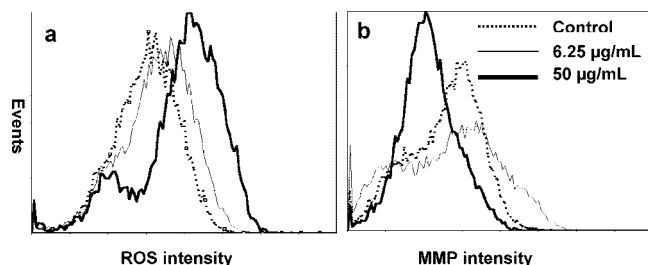


**Figure 5.** Flow cytometric analysis of dichlorofluorescein diacetate (H<sub>2</sub>DCF-DA for ROS) and Mitotracker Green FM (mitochondrial membrane potential) fluorescence by **1** in LNCaP cells. Increase of ROS production (a) and a loss of mitochondrial membrane potentials (b) by LNCaP cells after treatment with 6.25 and 50 µg/mL **1** for 30 min and 18 h, respectively.

(Figure 5b). The flow cytometric results together with those from immunoblotting and immunofluorescence microscopy indicate that oxidative stress and mitochondrial dissipation are likely involved in the apoptotic induction of **1**.

Apoptosis is a complex cascade that plays an important role in tissue homeostasis and development, and cancer development. Cells can be induced to apoptosis by either intracellular or extracellular inducers either through a death receptor-dependent pathway initiated by the interaction between a ligand and its receptor (e.g., FasL/FasL<sup>5</sup>) that activates caspase 8 or through a receptor-independent pathway that involves the generation of ROS, the dissipation of mitochondrial membrane potential, and translocation of cytochrome *c* from mitochondria into the cytosol for triggering apoptosis.<sup>4</sup> Regardless of the different types of apoptotic pathways, cells share an activation of a common executor, caspase 3, which results in the proteolysis of cellular components, DNA fragmentation, and formation of apoptotic bodies. In normal untreated LNCaP cells, the expression of procaspase 3, a caspase 3 precursor, was very weak, but increased significantly in the presence of **1** (6.25 and 25 µg/mL) for 48 h and remained elevated before the cells died at a dose of 50 µg/mL, as demonstrated by immunoblotting analysis (Figure S3, Supporting Information).

In order to investigate the pathway through which **1** mediated its apoptotic activities, cells were treated with 12.5 µg/mL **1** for one cell cycle (i.e., 48 h) for immunoblotting analysis of apoptosis-related proteins, p21, Fas, FasL, caspase 3, and caspase 8. All proteins were activated at various time points, and FasL peaked at 6 h, p21 around 12 h, and Fas at 24 h, while procaspase 8 increased constitutively for 48 h (Figure 6a). In a comparison between treatments with 12.5 and 50 µg/mL **1**, both procaspases 3 and 8 (32 and 55 kDa, respectively) were cleaved into active forms (23 kDa for caspase 8 and 12, 17, and 19 kDa for caspase 3) in both a time- and a dose-dependent manner. Consistent with cell death observation in immunofluorescence and immunoblotting analyses, the expression of both caspases decreased after 48 h exposure at the highest dose used (50 µg/mL) (Figure 6b).

Results obtained from a combination of immunoprecipitation and immunoblotting analysis of **1**-mediated apoptotic LNCaP cells using antibodies against p21 and Fas revealed an association of cyclin D and procaspase 3 with p21 (Figure 7a), while procaspase 3 was associated with Fas. The level of Fas was increased in a dose-dependent manner (Figure 7b). It is believed that ligation of Fas leads to receptor trimerization and assembly of a death-inducing signaling complex (DISC) involving association of Fas and two caspase precursors, namely, procaspase 8 and procaspase 3, for initiation of cell apoptosis.<sup>24,25</sup> Three proteins of molecular masses 55, 48, and 33 kDa, corresponding to procaspase 3, procaspase 8, and Fas receptor, were identified by MALDI-TOF mass spectrometry coupled with Uniprot/SWISSPROT. Together with a partial block of **1**-mediated apoptosis by pretreatment with antisense FasL oligonucleotide (8 µg/mL) for 2 h (data not shown), results of Fas/

caspases assembly strongly indicated a Fas–caspase 8–caspase 3 apoptotic pathway was involved in the cytotoxicity of **1**.

## Experimental Section

**Test Compound.** Neochamaejasmin A (**1**) (CAS Registry No. 90411-13-5) is a biflavonone with a C-3/C-3' linkage isolated from an 95% EtOH extract of the dried roots of *Stellera chamaejasme* L. (Thymelaeaceae), as previously described.<sup>12,13</sup> Briefly, the dried plant material (4 kg) was extracted with 95% EtOH. After removal of excessive solvent, the residue was successively extracted with petroleum ether, EtOAc, and EtOH. The EtOAc fraction was repeatedly chromatographed to yield a crop of neochamaejasmin A (**1**, 185 mg). The structure was identified by comparing the physical and spectroscopic data with literature values.<sup>12,13</sup> It has a molecular formula of C<sub>30</sub>H<sub>22</sub>O<sub>10</sub>, and the molecular weight is 542. The compound was dissolved in DMSO and diluted to appropriate concentrations with culture medium before use.

**Cell Culture.** The human prostate cancer cell line LNCaP (CRL-1740), the human colon cancer SW620 cell line (CCL227), and the mouse fibroblast L929 (CCL1) cell line were obtained from the American Type Culture Collection (ATCC, Rockville, MD). The cells were maintained routinely in RPMI supplemented with 10% fetal bovine serum (FBS), 100 µg/mL streptomycin, and 100 IU/mL penicillin at 37 °C in a humidified atmosphere of 5% CO<sub>2</sub>.<sup>11</sup>

**Cytotoxicity Assay.** Cancer cells (1 × 10<sup>4</sup> cells/0.1 mL/well) were incubated in the presence of serial dilutions of **1** in 96-well culture plates (Nunc, Roskilde, Denmark) or on eight-chamber culture slides (Nunc, Naperville, IL) for 48 h for the MTT (3-[4,5-dimethylthiazol-2-yl]-2,5-diphenyltetrazolium bromide) cytotoxicity assay. Data points represent the mean values and standard deviations of triplicate samples. IC<sub>50</sub> values were expressed as the concentration of **1** showing 50% formazan absorbance of the control group. Since LNCaP cells were the most susceptible cells to treatment with **1** after initial screening, they were pulsed with 0.5 µCi/10 µL/well of <sup>3</sup>H-thymidine (<sup>3</sup>H-Tdr, specific activity 5 µCi/mmol, Amersham, UK) for analysis of antiproliferative activity or cultured on the chamber slide and stained with acridine orange for morphological and apoptotic studies.<sup>11</sup>

**Immunofluorescence Microscopy.** Treated LNCaP cells were fixed with buffered formalin for both morphological and immunofluorescence analysis as described previously. For morphological observation, the cells were then stained with 0.01% acridine orange and differentiated with 0.1 M calcium chloride. Immunoreactive nucleolin and caspase 3 proteins were localized in treated cells using rabbit polyclonal antibodies against nucleolin and caspase 3 (Santa Cruz Biotechnology, Inc., Santa Cruz, CA) and the biotin–avidin fluorescence complex (Vector Laboratories, Burlingame, CA) prior to analysis on a fluorescence microscope (Axioskop, Zeiss, Germany).<sup>11</sup>

**Electron Microscopy.** Ultrastructural changes induced by **1** were examined using both scanning and transmission electron microscopy with LNCaP cells fixed in 2% glutaraldehyde and 0.1% OsO<sub>4</sub>. After washing in distilled water, the preparations were dehydrated through a graded series of ethanol, critical point dried with liquid CO<sub>2</sub>, and coated with platinum–gold, before the changes of cell surface structure were recorded using a JEOL JSM-35 scanning electron microscope. Another portion of dehydrated cells was embedded in Epon, sectioned, and stained with lead citrate and uranylacetate for transmission electron microscopic analysis (Hitachi 7100 electron microscope).

**Cell Cycle Analysis.** LNCaP cells were cultured in the presence of a serial dilutions of **1** for 48 h, or 6.26 µg/mL for 6 days, before the cells were fixed in 70% cold ethanol, resuspended in 1 mL of PBS containing 200 µg/mL RNase A (Sigma) and 20 µg/mL propidium iodide (PI, Sigma) at room temperature for 15 min. The red fluorescence of DNA-bound PI in individual cells was measured at 620 nm on a Coulter ALTRA flow cytometer. The results obtained from 10 000 cells were analyzed using Expo II software (Beckman Coulter Company).<sup>26</sup>

**Measurement of ROS Production.** Generation of intracellular ROS by **1**-treated LNCaP cells was measured with the fluoroprobe 2',7'-dichlorodihydrofluorescein diacetate (H<sub>2</sub>DCF-DA, Molecular Probes, Inc., Eugene, OR) as described previously.<sup>27</sup> The H<sub>2</sub>DCF-DA that converted to the green fluorescent product DCF by intracellular ROS was measured by flow cytometry (Coulter ALTRA flow cytometer) with excitation at 488 nm and emission at 535 nm, and the results were analyzed using Expo II software.

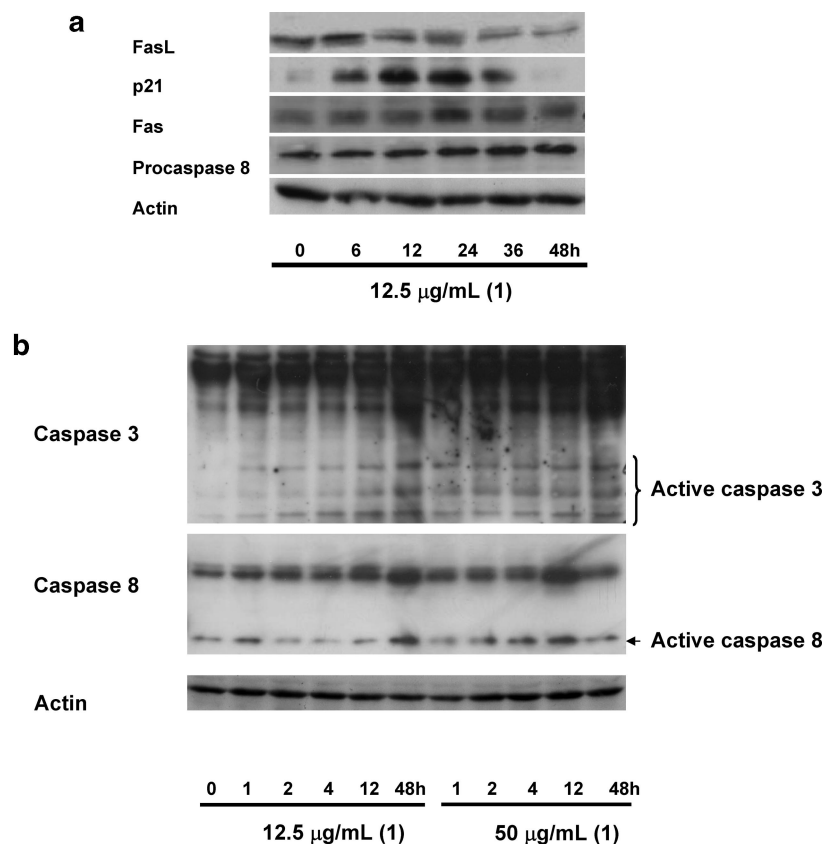


**Figure 6.** Immunoblotting analysis of apoptotic proteins shown in LNCaP cells after treatment with **1**. Equal amounts of proteins in the cell lysate from each treatment group were subjected to gel electrophoresis and immunoblotted with antibodies against FasL, Fas, p21, and caspase-8. All proteins significantly ( $p < 0.05$ ) increased at various time points, FasL peaked at 6 h, p21 around 12 h, and Fas at 24 h, while procaspase 8 increased constitutively between 36 and 48 h (a). Both caspase 3 and caspase 8 were significantly ( $p < 0.05$ ) activated in a dose- and a time-dependent manner (b).

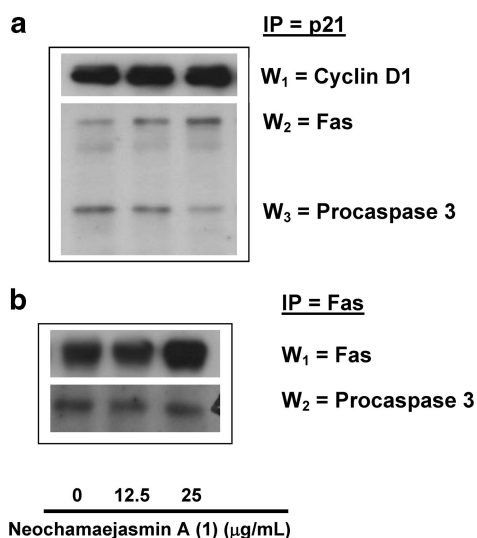


**Figure 7.** Immunoprecipitation assays showing LNCaP cells were treated with 12.5 and 25 µg/mL **1**, respectively, for 12 h, and the cell lysates were immunoprecipitated with antibodies against p21 and Fas for immunoblotting analysis and MALDI-mass spectrometric protein identification. Immunoreactive cyclin D, Fas, and procaspase 3 were found associated with p21 (a), while procaspase 3 was associated with Fas, and the levels of Fas itself were also increased in a dose-dependent manner (b).

**Determination of Mitochondrial Transmembrane Potential.** The mitochondrial membrane potential of **1**-treated LNCaP cells was measured using a mitochondrion-specific probe, Mitotracker Green FM (MTG, Molecular Probes, Inc.), according to the method described in

a previous paper.<sup>27</sup> Briefly, LNCaP cells were treated with serial concentrations of **1** for 18 h. During the last 15 min, cells were incubated with 100 nM MTG in culture medium at 37 °C in the dark before they were rinsed with PBS and subsequently subjected to flow cytometric analysis with excitation at 490 nm and emission at 510 nm. The results were analyzed using Expo II software.

**Transcription of the p21 Gene.** Total cellular RNA was isolated from LNCaP cells ( $5 \times 10^6$  cells) using Trizol reagents, and 1 µg of each sample was directly reverse-transcribed to cDNA for PCR using Thermoprime DNA polymerase and primers against p21 (forward 5'-CTTTGACTTCGTCACGGAGAC-3' and reverse 5'-AGGCAGCGTATATCGGAGAC-3') (GIBCO/BRL) in a 9700 Perkin-Elmer thermal cycler. The PCR products were separated on a 1.2% agarose gel, and band intensity was measured by a Chemiluminescence Imaging Analysis System with FluorChem software (Alpha Innotech Corp., San Leandro, CA). The intensity of each band was normalized to that of the internal control,  $\beta$ -actin (forward 5'-CCTTCTACAATGAGC-3' and reverse 5'-ACGTCACACTTCATG-3').<sup>11</sup>

**Immunoblotting Analysis.** Total cell lysate was collected from LNCaP cells treated with **1** and normalized for protein content using the BCA protein assay reagent (Pierce, Biotechnology Inc., Rockford, IL). Equal amounts of protein samples were separated on a 12% SDS-PAGE gel and transferred onto a PVDF membrane for immunoblotting analysis with polyclonal antibodies against (1) apoptosis-related proteins Fas and FasL (Santa Cruz Biotechnology) and rabbit antiserum to caspase 8 (Pharmingen) and caspase 3 (Santa Cruz Biotechnology), and (2) cell cycle regulatory proteins mouse monoclonal antibody to cyclin D (Santa Cruz Biotechnology), mouse monoclonal antibody to proliferating cell nuclear antigen (PCNA, Santa Cruz Biotechnology), and mouse monoclonal antibodies to cyclin-dependent kinase inhibitor, p21 (Santa Cruz Biotechnology), followed by the horseradish peroxidase (Tago)-enhanced chemiluminescence system. The amounts of translational proteins were analyzed and normalized with actin (Neomarker, Fremont, CA) using a FluorChem Imager.<sup>28</sup>

**Electrophoretic Mobility Shift Assay (EMSA).** EMSA was used to detect specific DNA binding of transcription factors (NF $\kappa$ B and AP-1) in LNCaP cells treated with **1**. Briefly, nuclear extracts were prepared from treated LNCaP cells using the NE-PER nuclear extraction reagent (Pierce Biotechnology), and the electrophoretic mobility shift assay (EMSA) for binding of nuclear proteins to the cyclin D-specific sequences of NF $\kappa$ B (5'-GATCGAGGGGACTTCCCTAGC-3') and AP-1 (5'-CTAGTGATGAGTCAGCCGGATC-3') (Syngen, Inc., Belmont, CA) was carried out as described previously.<sup>28</sup>

**Immunoprecipitation, Immunoblotting, and Mass Spectrometry.** To examine a direct involvement of p21 in growth arrest and Fas-mediated apoptosis, total cell lysate from **1**-treated LNCaP cells was incubated with primary antibodies against Fas or p21, and protein A Sepharose beads (Amersham BioSciences, Uppsala, Sweden) to form a target protein complex with protein A beads. After washing, the bound proteins were removed from the beads and resolved by 12% SDS-PAGE before they were transferred onto a PVDF membrane for immunoprobining with antibodies against cyclin D, Fas, and caspase 3 for p21-associated proteins and against Fas and caspase 3 for Fas-associated proteins, and the reactive proteins were detected by enhanced ECL and Lumi film (Roche, Mannheim, Germany).

A duplicated set of SDS-PAGE gels was stained with coomassie blue, and the respective proteins were dissected for in-gel trypsin digestion at 37 °C overnight for mass spectrometry.<sup>29</sup>

**Involvement of FasL in Cytotoxicity of **1** by Antisense Oligonucleotide Treatment.** LNCaP cells ( $3 \times 10^5$  cells/well/mL) were preincubated with 8  $\mu$ g/mL phosphorothioate-modified sense (5'-AGCTGGCAGAACTCCGAGAG-3') and antisense FasL oligonucleotide (5'-CTCTCGGAGTTCTGCCAGCT-3')<sup>26</sup> (Syngen, Inc.) in 3  $\mu$ L of lipofectamine (Invitrogen, Carlsbad, CA) for 2 h before they were challenged with 50  $\mu$ g/mL **1** for 24 h. The cells were collected for cell viability evaluation by the trypan blue exclusion method.

**Statistical Analysis.** Data were analyzed by one-way analysis of variance (except comparison of cytotoxicity among three cell lines with two-way analysis of variance) followed by Duncan's multiple range test to detect intragroup (intergroup for two-way analysis) differences using GraphPad Prism software 5.0. Significant differences were considered at  $p < 0.05$  (\*) and  $p < 0.001$  (\*\*\*)

**Acknowledgment.** The authors would like to thank Dr. K. W. Li, Dr. P. Ip, Mr. S. Wong, Miss V. W. Chow, and Miss Q. Wang for technical assistance. The work described in this paper was supported partially by a grant from the Hong Kong Research Grants Council (Project No. CUHK4169/99M).

**Note Added after ASAP Publication:** The version posted on April 2, 2008, was missing the structure **1** graphic. Structure **1** appears in the version posted on April 11, 2008.

**Supporting Information Available:** Apoptotic changes of treated cells by scanning and transmission electron microscopy; flow cytometric analysis of **1**-mediated cell arrest and apoptosis; and epifluorescence microscopy, immunofluorescence, and immunoblotting analysis of procaspase 3 expression and nucleolin in **1**-treated cells are provided free of charge via the Internet at <http://pubs.acs.org>.

## References and Notes

- Gleave, M.; Qian, J.; Andreou, C.; Pommerville, P.; Chin, J.; Casey, R.; Steinhoff, G.; Fleshner, N.; Bostwick, D.; Thomas, L.; Rittmaster, R. *Prostate* **2006**, *66*, 1674–1685.
- Muenchen, H. J.; Ponca, P. J.; Pienta, K. J. *Urology* **2001**, *57*, 366–370.
- Petronilli, V.; Penzo, D.; Scorrano, L.; Bernardi, P.; Di Lisa, F. *J. Biol. Chem.* **2001**, *276*, 12030–12034.
- Khosravi-Far, R.; Esposti, M. D. *Cancer Biol. Ther.* **2004**, *3*, 1051–1057.
- Boatright, K. M.; Salvesen, G. S. *Curr. Opin. Cell Biol.* **2003**, *15*, 725–731.
- Yang, C. L. *Materia Medica of Toxic Herbs*; Chinese Medicine and Materials Publisher: Beijing, 1993; pp 1021–1023.
- Ma, Q. G.; Liu, W. Z.; Wu, H. M.; Zhou, T. X.; Qin, G. W. *Phytochemistry* **1997**, *44*, 663–666.
- Che, C. T.; Ma, Q. G.; Qin, G. W.; Williams, I. D.; Wu, H. M. *Phytochemistry* **1999**, *52*, 117–121.
- Lee, S. H.; Tanaka, T.; Nonaka, G. I.; Nishioka, I.; Zhang, B. *Phytochemistry* **1991**, *30*, 1251–1253.
- Tu, S. J.; Wang, P.; Wei, A. *Chin. J. Integr. Trad. West. Med.* **1984**, *4*, 46–47.
- Liu, W. K.; Ho, J. C. K. *Biochem. Pharmacol.* **2002**, *63*, 951–957.
- Liu, X.; Ye, W.; Che, C. T.; Zhao, S. *Zhongcaoyao* **2003**, *34*, 399–401.
- Niwa, M.; Tatematsu, H.; Liu, G.; Hirata, Y. *Chem. Lett.* **1984**, *148*, 539–542.
- Kim, H. K.; Son, K. H.; Chang, H. W.; Kang, S. S.; Kim, H. P. *Arch. Pharm. Res.* **1999**, *21*, 406–410.
- Banerjee, T.; Valacchi, G.; Ziboh, V. A.; van der Vliet, A. *Mol. Cell. Biochem.* **2002**, *238*, 105–110.
- Farombi, E. O.; Moller, P.; Dragsted, L. O. *Cell. Biol. Toxicol.* **2004**, *20*, 71–82.
- Kito, S.; Shimizu, K.; Okamura, H.; Yoshida, K.; Morimoto, H.; Fujita, M.; Morimoto, Y.; Ohba, T.; Haneji, T. *Biochem. Biophys. Res. Commun.* **2003**, *300*, 950–956.
- Coqueret, O. *Gene* **2002**, *299*, 35–55.
- Kontopidis, G.; Wu, S. Y.; Zheleva, D. I.; Taylor, P.; McInnes, C.; Lane, D. P.; Fischer, P. M.; Walkinshaw, M. D. *Proc. Natl. Acad. Sci. USA* **2005**, *102*, 1871–1876.
- Nakamura, K.; Arai, D.; Fukuchi, K. *Arch. Biochem. Biophys.* **2004**, *431*, 47–54.
- Andreassen, P. R.; Lacroix, F. B.; Lohez, O. D. *Cancer Res.* **2001**, *61*, 7660–7668.
- Bharti, A. C.; Aggarwal, B. B. *Biochem. Pharmacol.* **2002**, *64*, 883–888.
- Napoli, C.; de Nigris, F.; Palinski, W. J. *Cell. Biochem.* **2002**, *82*, 674–682.
- Suzuki, A.; Suzuki, Y.; Tsutomi, N.; Yamamoto, T.; Shibutani, K.; Akahane, K. *Mol. Cell. Biol.* **1999**, *19*, 3842–3847.
- Suzuki, A.; Tsutomi, Y.; Akahane, K.; Araki, T.; Miura, M. *Oncogene* **1998**, *17*, 931–939.
- Liu, W. K.; Ho, J. C. K.; Cheung, F. W. K.; Liu, B. P. L.; Ye, W. C.; Che, C. T. *Eur. J. Pharmacol.* **2004**, *498*, 71–78.
- Liu, W. K.; Ho, J. C. K.; Ng, T. B. *Biochem. Pharmacol.* **2001**, *61*, 33–37.
- Sze, S. C. W.; Ho, J. C. K.; Liu, W. K. *J. Cell. Biochem.* **2004**, *92*, 1193–1202.
- Li, K. W. <http://www.bio.vu.nl/vakgroepen/mnb/frs1/ proteomics.html>. NP8001223